Analysis of Water Flow under Trickle Irrigation: II. Experimental Evaluation

F. Lafolie, R. Guennelon, and M. Th. van Genuchten*

ABSTRACT

A numerical solution for predicting soil water content distributions during trickle irrigation on stratified and anisotropic soils was compared with data from a field experiment carried out on a loamy clay soil using 24 field plots irrigated at different rates and frequencies. The unsaturated hydraulic conductivity was estimated from measured soil water retention and saturated hydraulic conductivities. Observed volumetric soil water contents and saturated areas on the soil surface were compared with model predictions. The effects of anisotropy and soil surface crusting on experimental and calculated soil water distributions were also investigated. Relatively good agreement was obtained between predicted and measured soil water content distributions vs. depth. The shape of the observed wetted soil volume was also predicted reasonably well. The effects of possible errors in the hydraulic characteristics on calculated water content distributions are discussed.

INCREASED IRRIGATION EFFICIENCY and reduced water stress are some of the factors that have contributed to the increased popularity of trickle (drip) irrigation during the last several decades (Bucks et al., 1982, p. 220–290). A quantitative understanding of soil water distributions during trickle irrigation is needed for optimizing crop production and minimizing deep percolation losses of water. This understanding may be developed through a combination of field experimentation and numerical modeling.

Until now, most published experimental data for evaluating trickle irrigation models have been for relatively coarse-textured soils, since trickle irrigation initially was developed mainly for this type of soils in arid and semi-arid areas (e.g., Israel and the southwestern U.S.A.). By contrast, experimental data for fine-textured soils are nearly absent (Mostaghimi et al., 1983). The purpose of this work is to describe a trickle irrigation field experiment conducted on a layered clay soil, and to compare the experimental data with results from a numerical finite difference model described by Lafolie et al. (1989).

F. Lafolie and R. Guennelon, Station de Science du Sol, INRA, Domaine St-Paul, B.P. 91, 84140 Montfavet, France; M.Th. van Genuchten, USDA-ARS, U.S. Salinity Lab. 4500 Glenwood Drive, Riverside, CA 92501. Received 2 May 1988. *Corresponding author.

Published in Soil Sci. Soc. Am. J. 53:1318–1323 (1989).

MATERIALS AND METHODS

Field Experiments

The experiments were carried out on a 1-ha field at the INRA station in Montfavet, France. A geostatistical analysis of observed particle size distributions revealed little variation in surface soil texture across the field. The mean particle size distribution was found to be 29% clay, 60% silt and 11% sand. Twenty four equally spaced drippers were located

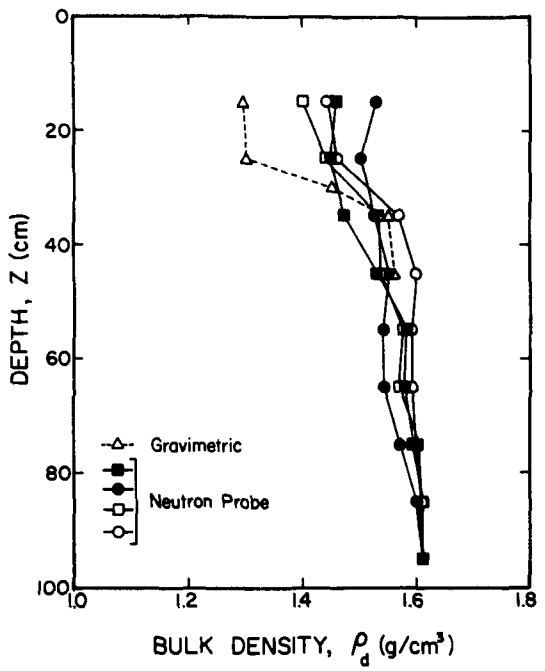

Fig. 1. Measured vertical bulk density distributions at selected points along the trickle irrigation line.

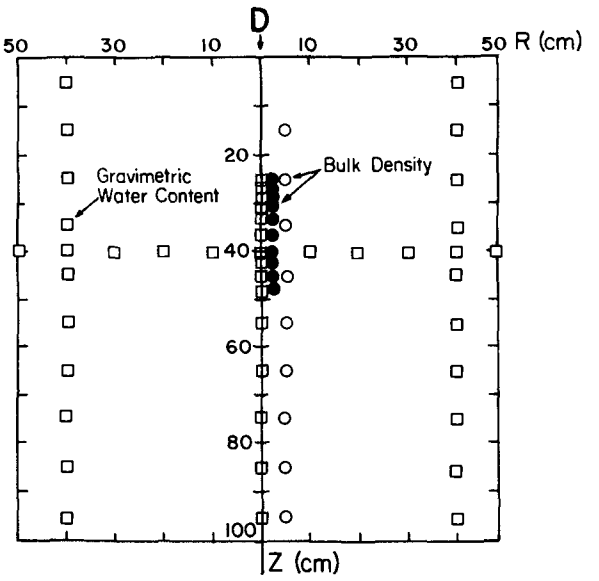

Fig. 2. Sampling locations for soil bulk density and gravimetric water content measurements in a vertical cross section under the dripper (D).

along a 70-m-long trickle line. The discharge rates of the drippers were all approximately 4L/h as measured before and after each irrigation. For time and technical reasons, the experiments were conducted successively on sets of, at most, five drippers. Each plot corresponding to a single dripper was first carefully leveled and then irrigated following a schedule that involved cycles of approximately 4 h of irrigation and close to 20 h of redistribution.

Four vertical neutron-probe access tubes were installed at regular intervals along the trickle line for the purpose of estimating soil bulk density profiles by neutron scattering. Another bulk density profile was obtained gravimetrically by sampling successive soil cores between 0 and 130 cm. Results are plotted in Fig. 1. Notice a relatively sharp transition zone in bulk density at around the 30-cm depth, especially for the gravimetric sampling. The transition is less apparent for the neutron method, since sharp changes with this method are smoothed by averaging over relatively large volumes of soil. Because of the observed bulk density change at 30 cm, the soil profile was assumed to consist of two layers, each having its own hydraulic properties.

Data Recorded for Each Plot

Initial water-content profiles were obtained by taking core samples adjacent to each plot at 10-cm intervals until a depth of 1 m. Photographs of the soil surface under each dripper taken at the end of the last irrigation were used to estimate both the saturated and unsaturated wetted areas at the soil surface. The photographs were also used to verify the shape of the ponded areas (circular or otherwise).

A large number of data was recorded at several sampling locations (Fig. 2), 2 to 5 h after the end of the last irrigation. First, the axis of symmetry of each plot was established (usually just below the dripper), at which location a soil bulk-density profile between 25- and 45-cm depth at 3-cm intervals was measured by gamma-ray transmission. Next, a vertical trench was carefully cut through the axis of symmetry, and samples taken for gravimetric soil water content measurements. Figure 2 shows the location of these water-content measurements, i.e., along a vertical line below the dripper between the gamma-ray access tubes, along vertical lines 40 cm away from the dripper, and also along a horizontal line at 40-cm depth. The data were used to estimate spatial distributions of the water content, and to assess the dimensions of the wetted soil volume.

Determination of the Soil Hydraulic Characteristics

The soil water content (θ)-pressure head (ψ) relationship in the range of 0 to -150 m was obtained using pressure cells. One field plot was equipped with five tensiometers at depths of 20, 40, 60, 80 and 100 cm, and with a neutron-probe access tube for water content measurements. The field-measured soil water retention curve between 0 and -800 cm was in good agreement with the laboratory measured curve. No significant differences between the gravimetric retention curves were found for the surface and subsurface horizons. Attempts to fit the analytical expressions of Brooks and Corey (1964) or van Genuchten (1980) to the observed data were not very successful. Consequently, we smoothed the data with a cubic spline function and used the resulting curve to generate a vector of 200 retention points at intervals ($\Delta\theta$) of 0.0025. The derivative of the spline function was used to generate corresponding soil water capacities. Linear interpolation between the entries of the water retention vector was used during the numerical simulations.

The saturated hydraulic conductivity, K_s, was measured at seven regularly spaced locations along the trickle irrigation line for the upper layer, and at five locations for the second layer. Measurements were made on soil cores (15-cm diam., 7-cm height) taken immediately after the last irrigation. The cores were taken with metal cylinders that were driven into the wetted zone under the emitters. The two ends of the samples were then carefully smoothed while, at the same time, avoiding any slaking of the soil. In the laboratory, these samples were slowly wetted from below to reduce air entrapment. Once saturated, different positive total pressure heads in the range of 0.1 to 5 cm were imposed at the bottom of the sample. After establishing steady-state flow, the corresponding flow rates were recorded. A linear regression between the measured fluxes and potential dif-

Table 1. Measured saturated conductivities, K_s, of the surface and subsurface soil layers.

Surface layer (0–30 cm)		Subsurface layer (>30 cm)	
Site no.	K_s	Site no.	K_s
	m d^{-1}		m d^{-1}
1	3.14	1	0.86
2	3.64	2	0.95
3	14.7	3	0.09
4	2.95	4	2.94
5	24.5	5	0.29
6	2.75		
7	3.09		

ferences gave the global resistance of the system consisting of the soil sample plus attached permeameter. Subtracting the known resistance of the permeameter gave the resistance of the soil, and hence the hydraulic conductivity as the inverse of the resistance. The linear regressions over seven or eight points were always excellent, giving intercepts that were generally very close to zero. Values for K_s measured in this manner are listed in Table 1. Notice that, except for two samples that probably contained some macropores, K_s for the surface layer remained in a relatively narrow range between 2.7 and 3.7 m/d. By comparison, results for the second layer were more scattered. Having data for the soil water retention curve and K_s, the predictive pore size distribution model of Mualem (1976) was subsequently used to estimate the unsaturated hydraulic conductivity curve, $K(\psi)$, for the two soil layers. For each simulation, we always used the measured conductivity value of the nearest sampling site.

Modification of the Predicted Hydraulic Conductivity Curve

Figure 3 shows that the measured soil water retention curve decreases very quickly between saturation and the first measured data point less than saturation. Because of this, Mualem's model generated a $K(\psi)$-curve which decreased very sharply when ψ became <0. For example, between $\psi = 0$ and -15 cm, the hydraulic conductivity decreased by a factor of 10^4 (Fig. 4). For similar reasons, the soil water capillary capacity, $d\theta/d\psi$, close to saturation was also very high. Simulations made with these hydraulic curves resulted in water content profiles with extremely large gradients (sharp moisture fronts) which did not agree with the observed field data (results not shown here). These large gradients also persisted between individual irrigations, again being contrary to our observations. Because of the above inconsistencies, we decided to modify the Mualem-predicted hydraulic conductivity curve close to saturation. Figure 4 shows a semi-logarithmic plot of K/K_s vs. ψ. Note that the curve is more or less linear for ψ less than -30 cm. Because the first observed data point of the $\theta(\psi)$ curve less than saturation was at $\psi = -30$ cm, we decided to use the predicted $K(\psi)$ curve only for ψ values less than -30 cm. Between 0 and -30 cm we adopted, rather arbitrarily, an exponential relation of the form $K = K_s \exp(\beta\psi)$, where β was calculated to keep continuity at $\psi = -30$ cm (see the dashed line in Fig. 4). No independent laboratory data were available to support this modification, and hence the accuracy of the modified curve could not be further assessed.

RESULTS AND DISCUSSION

Figure 5 compares calculated and observed vertical water content distributions immediately under the dripper, and at a radial distance of 40 cm. Similar

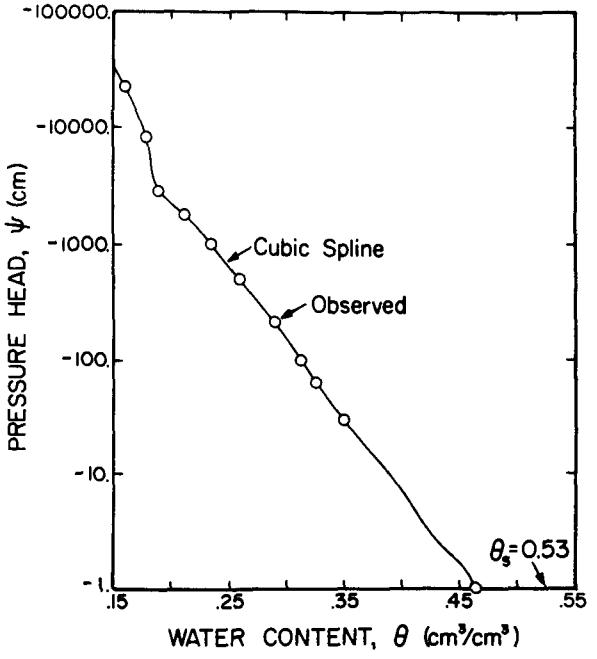

Fig. 3. Observed and cubic spline soil water retention curves, $\psi(\theta)$, for the surface soil layer, 0 to 30 cm.

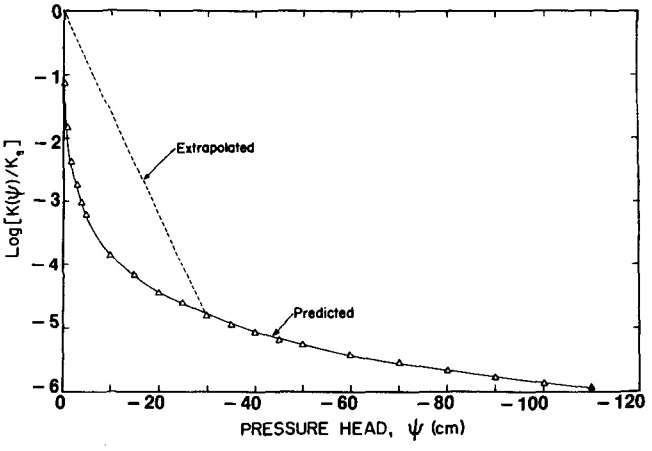

Fig. 4. Semi-logarithmic plot of the relative hydraulic conductivity, K/K_s, vs. pressure head, ψ, as predicted with Mualem's model (solid line) and interpolated from saturation to the first data point of the measured soil water retention curve (dashed line).

horizontal distributions at 40-cm depth are given in Fig. 6. Observed results are averages of four or five replicates, with the bar through each data point indicating the range of observed values. The data were taken after 66 (top), 92 (middle) and 165 (bottom) hours of irrigation, corresponding to total amounts of applied water of 56, 64, and 107 L, respectively. The extremely low initial water contents near the soil surface corresponded to a pressure head of less than -100 m.

The calculated water content distributions in Fig. 5 and 6 (solid lines) were obtained with the numerical model of Lafolie et al. (1989). Numerical results were obtained for a domain extending 75 cm radially and 130 cm vertically. Vertical increments of the finite difference grid increased from 2 cm at the soil surface to 4 cm at the bottom of the domain, while the radial

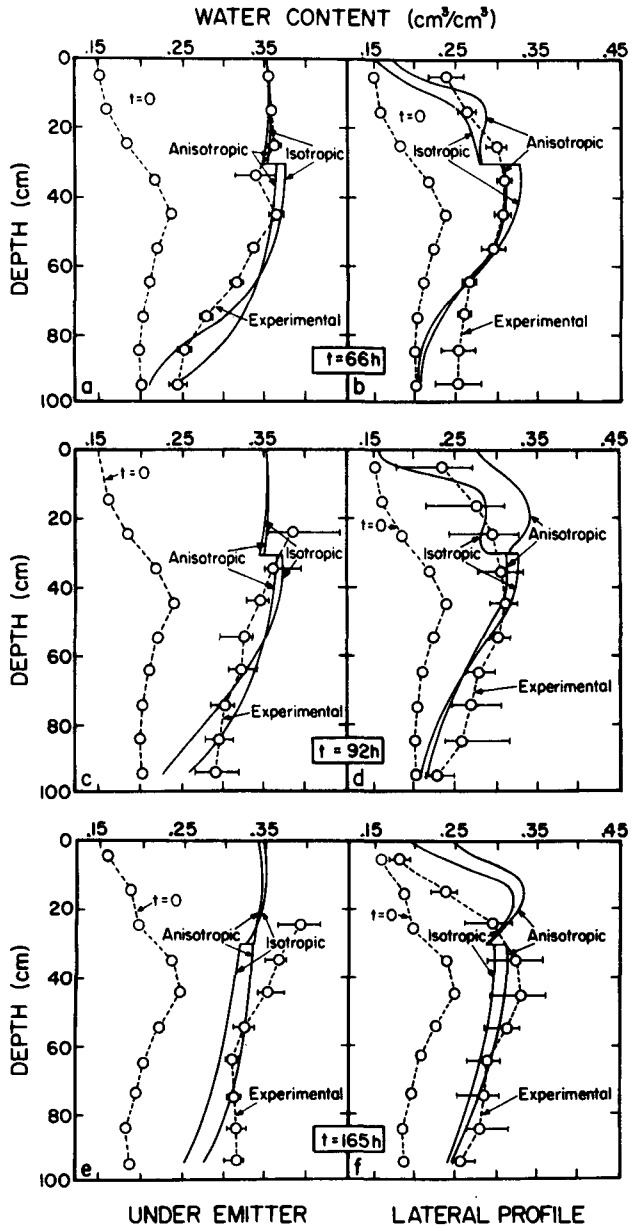

Fig. 5. Measured and calculated water content distributions under the dripper (left) and at a radial distance of 40 cm away from the dripper (right), after application of 56 (a,b), 64 (c,d) and 107 L (e,f) of water. Calculations are for an isotropic and anisotropic conductivity tensor.

increments were 3 cm. The time step varied from 1 s to 1 h. The simulations were initially carried out with an isotropic hydraulic conductivity tensor. Figure 5 and 6 show reasonable agreement between the field-measured data and the simulated results. However, some systematic discrepancies existed. For example, the calculated vertical water content distributions at a radial distance of 40 cm were always lower than those measured in both the extreme top and bottom parts of the soil profile (Fig. 5b,d,f). The same is true for the water content in the bottom of the profile just below the dripper (Fig. 5a,c,e).

Several factors probably contributed to these deviations. For example, the experimental water content distributions were derived from observed gravimetric

Table 2. Measured and calculated saturated radius, R_s, for isotropic and anisotropic soil crusting conditions.

Time	Measured†	Calculated	
		Isotropic	Anisotropic
h	cm	cm	
66	9, 11, 9, 10	7.8	16.0
92	16, 16, 18	8.0	17.5
165	19, 20, 27, 27	8.2	17.0

† Values of replicates.

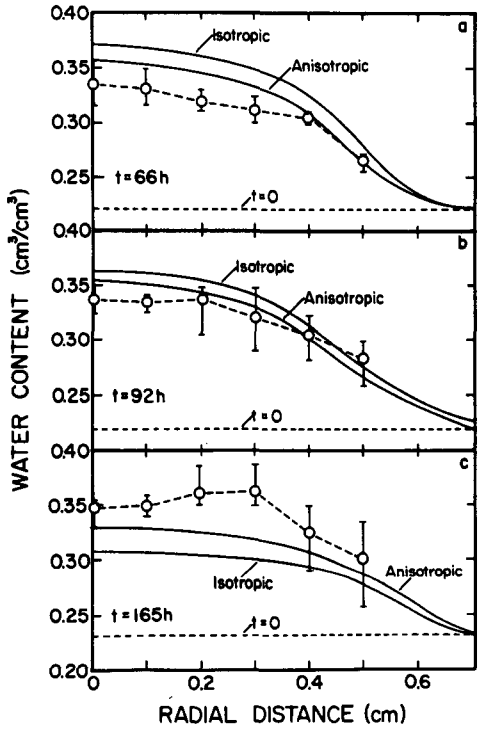

Fig. 6. Measured and calculated horizontal water content distributions at the 40-cm depth. Calculations are for an isotropic and anisotropic conductivity tensor.

values using measured bulk densities (ρ_d) at the corresponding depths, whereas a constant ρ_d was assumed for each of the two layers in the simulations (1.33 and 1.54 g/cm³ for the surface and subsurface layers, respectively). Measured ρ_d at depths greater than 90 cm always exceeded 1.6, resulting in local errors in water contents up to about 6%. We also noticed an increase in ρ_d of the top layer during the experiments as a function of the amount of applied water. Gamma-probe data recorded for each plot showed that, at the end of the experiments, the average dry ρ_d had increased to about 1.45 in the surface layer. This caused additional deviations of up to about 10% in the calculated water content.

Table 2 compares observed and predicted values of the saturated radius, R_s, at the soil surface. Except for the first sampling at $t = 66$ h, calculated results for the isotropic case severely underpredicted the measured values. We believe that these deviations between observed and predicted R_s values, as well as those between the observed and predicted water content in Fig. 5 are caused primarily by the relatively poor characterization of the soil hydraulic properties.

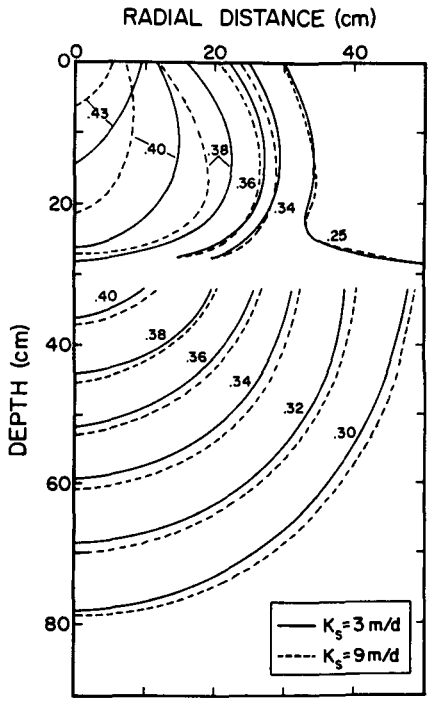

Fig. 7. Effect of the saturated hydraulic conductivity, K_s, of the surface horizon on calculated water-content distributions during trickle irrigation.

Several factors, in addition to those mentioned above, likely played a role. We initially hypothesized that the saturated conductivity, K_s, of the surface layer might have been overestimated during at least part of the experiments. To test the effect of changes in K_s of the surface layer, we carried out several simulations. Figure 7 presents the results obtained for a 4-h trickle irrigation with the same soil as before, but now for a uniform initial pressure head of -500 cm. Results are for two values of K_s of the surface horizon, 3 and 9 m/day, leading to saturated radii of 7.2 and 4.0 cm, respectively. As expected, the smaller K_s value resulted in a larger wetted radius, R_s. However, the water content distributions inside the profile were only marginally affected by the change in K_s of the surface layer. This is especially true for the water contents in the deeper soil layers. Similar effects were found when the entire experiment, as in Fig. 5, was simulated. Hence, improved water content distributions in the soil profile could not be obtained by simply changing the saturated hydraulic conductivity of the surface layer.

During the field experiments, we observed the formation of a thin soil surface crust that more or less followed the ponded area on the soil surface below the dripper. Formation of a soil crust is presumably caused by particle dispersion and/or soil swelling during saturated or near-saturated flow, and will result in lower porosities and hydraulic conductivities, especially for fine-textured soils (Shainberg and Shalhevet, 1984). The main effect of soil crust formation in our experiments was to increase the saturated (ponded) area with each irrigation cycle, as indeed shown by the data in Table 2. Similar effects of soil sealing and possibly compaction were noted by Jury and Earl (1977) during a series of field experiments on a sandy loam soil. These authors also found that successive laboratory measurements of K_s tended to give lower values, further indicating that pore geometry was changing with time.

Another factor which may have caused a discrepancy between observed and predicted water contents is anisotropy in the hydraulic conductivity tensor. In situ observations of the wetted soil profile along the walls of open soil trenches indicated the presence of preferential flow paths in the soil. Preferential flow paths were especially visible in the well-structured subsurface horizon at depths greater than 30 cm. As shown by Wang and Narasimhan (1985), gravity induced preferential flow may occur in a structured soil, even when water contents are slightly less than saturation. One way to numerically account for preferential flow in a structured soil is to assume an anisotropic hydraulic conductivity tensor in which the saturated hydraulic conductivity in the vertical direction ($K_{v,s}$) is larger than the horizontal saturated hydraulic conductivity ($K_{h,s}$).

In order to test the above assumptions, we incorporated provisions for surface crusting and soil anisotropy into the numerical model. The time-dependent nature of the soil-crusting process at the soil surface was approximated by multiplying K_s of the surface 2 mm of soil under the dripper by a "soil-crusting factor" (c_f) of 0.2 once the soil became saturated. In accordance with field observations, only the saturated soil surface was assumed to be affected by soil crusting. The value of $c_f = 0.2$ was chosen such that it reduced K_s significantly from its original value, while still yielding values that are considerably higher than K_s values typical for fully developed soil crusts (Shainberg and Shalhevet, 1984). Anisotropy in the hydraulic conductivity was approximated by increasing $K_{v,s}$ of the second (subsurface) layer by 50%.

Numerical results for the anisotropic soil-crusting case are also shown in Fig. 5. Predictions of the water contents in the subsurface layer were improved, although discrepancies remained in the deeper layers away from the axis of symmetry (Fib. 5b,d). Note that water contents of the surface horizon immediately below the emitter were essentially unaffected by surface crusting (Fig. 5a,c,d), whereas surface water contents at a radial distance of 40 cm from the dripper were higher. These higher water contents at $r = 40$ cm resulted from the larger ponded radii (Table 2) caused by soil crusting. The above effects of soil crusting and soil anisotropy can only be approximated because of inaccurate and incomplete data of the soil hydraulic properties in time and space. However, they do accurately reflect the qualitative effects of the crusting and preferential flow phenomena.

SUMMARY AND CONCLUSIONS

A previously proposed numerical model for predicting soil profile water content distributions during trickle irrigation on stratified and anisotropic soils (Lafolie et al., 1989) was used to analyze a field trickle irrigation experiment. The experiments were carried out on a loamy clay soil using 25 field plots irrigated

at different rates and frequencies. Results for a typical set of experiments involving cycles of 4 h of irrigation and 20 h of redistribution are presented in this paper.

While the observed water contents were simulated reasonably well with the model, a number of systematic discrepancies were noted. Most of these could be related to inadequate characterization of the unsaturated soil hydraulic conductivity. In our study, this soil property was estimated from the field-measured soil water retention curve using the predictive model of Mualem (1976). The estimated hydraulic conductivity curve was modified in the vicinity of saturation to allow for realistic predictions of the measured soil water contents. Other problems involving the hydraulic properties were related to the heterogeneous behavior of the fine-textured soil. For example, particle dispersion and/or soil swelling probably contributed to the formation of a thin soil crust on the soil surface under the emitter. As shown by numerical simulations, the associated reductions in porosity and hydraulic conductivity help to explain the larger than predicted saturated (ponded) areas observed on the soil surface during the experiments. Soil heterogeneity was also related to preferential flow in the well-structured subsurface horizon at depths greater than 30 cm. Preferential flow was accounted for by assuming an anisotropic hydraulic conductivity tensor which favors water flow in the vertical direction.

Inclusion of soil crusting and soil anisotropy resulted in improved predictions of soil water contents, and especially of the ponded area at the soil surface. We conclude that accurate descriptions of the soil hydraulic properties are crucial for reliable prediction of soil water contents during trickle irrigation. Accurate descriptions of the hydraulic properties appear especially important when calculated water fluxes are later used for predicting solute transport during trickle irrigation.

REFERENCES

Brooks, R.H., and A.T. Corey. 1964. Hydraulic properties of porous media. Hydrol. Pap. 3. Colorado State Univ., Fort Collins.

Bucks, D.A., F.S. Nakayama, and A.W. Warrick. 1982. Principles, practices, and potentialities of trickle (drip) irrigation. *In* Advances in irrigation. Vol. 1. Academic Press, New York.

Jury, W.A., and K.D. Earl. 1977. Water movement in bare and cropped soil under isolated trickle emitters. Soil Sci. Soc. Am. J. 41:852–856.

Lafolie, F., R. Guennelon, and M.Th. van Genuchten. 1989. Analysis of water flow under trickle irrigation. I. Theory and numerical solution. Soil Sci. Soc. Am. J. 53:1310–1318 (this issue).

Mostaghimi, S., and J.K. Mitchell. 1983. Pulse trickling effects on soil moisture distribution. Water Resour. Bull. 19:605–612.

Mualem, Y. 1976. A new model for predicting the hydraulic conductivity of unsaturated porous media. Water Resour. Res. 12:513–522.

Shainberg, I., and J. Shalhevet. 1984. Soil salinity under irrigation. Processes and management. Springer-Verlag, Berlin.

van Genuchten, M.Th. 1980. A closed-form equation for predicting the hydraulic conductivity of unsaturated soils. Soil Sci. Soc. Am. J. 44:892–898.

Wang, J.S.Y., and T.N. Narasimhan. 1985. Hydrologic mechanisms governing fluid flow in a partially saturated, fractured, porous medium. Water Resour. Res. 21:1861–1874.